Computers & Fluids, Vol. 1, pp. 251–271. Pergamon Press, 1973. Printed in Great Britain.

THE NUMERICAL SOLUTION OF THE NAVIER–STOKES EQUATIONS FOR LAMINAR INCOMPRESSIBLE FLOW PAST A PARABOLOID OF REVOLUTION

A. E. P. VELDMAN
Dept. of Mathematics, University of Groningen, the Netherlands

(*Received* 9 *February* 1973)

Abstract—A numerical method is presented for the solution of the Navier–Stokes equations for flow past a paraboloid of revolution. This method is based upon the ideas of van de Vooren and collaborators [1, 2]. The flow field has been computed for a large range of Reynolds numbers. Results are presented for the skinfriction and the pressure together with their respective drag coefficients. The total drag has been checked by means of an application of the momentum theorem.

1. INTRODUCTION

The numerical solution of the Navier–Stokes equations for laminar incompressible flow past a semi-infinite flat plate has been obtained by van de Vooren and Dijkstra [1]. Later, their method was improved and applied to the problem of flow past a parabolic cylinder by Botta, Dijkstra and Veldman [2]. In the present paper the axisymmetric viscous flow past a paraboloid of revolution is investigated.

The problem depends on a Reynolds number Re, which is based upon the semi nose radius of curvature of the paraboloid. The following three cases can be distinguished:

(i) $Re = 0$. This case corresponds to the semi-infinite needle which has no influence on any oncoming flow.

(ii) $Re \to \infty$. In this case the flow is governed by the boundary layer equations. These equations have been solved numerically by Smith and Clutter [3]. An approximate solution has been given by Davis [4] who has used a local series truncation method.

(iii) $0 < Re < \infty$. The governing equations then are the full Navier–Stokes equations. It is the purpose of this paper to cover this range of Reynolds numbers. A solution valid far downstream has already been given by Mather [5], Lee [6], Cebeci, Na and Mosinskis [7] and Miller [8, 9]. Tam [10] has proved the existence of such a solution for a heated paraboloid.

The basic idea of the methods used in [1] and [2] is the subtraction of the behaviour at infinity. With the aid of analytical arguments an expression is derived for the streamfunction and the vorticity valid for large values of the coordinates. The quantities used in the actual numerical calculations then are the deviations of the full solution from this asymptotic behaviour at infinity. Another important feature of the method is the transformation of the infinite region of interest to a finite region. This transformation is carefully adapted to the behaviour of the numerically calculated quantities. Using this method one obtains results for the full solution which are extremely accurate far downstream.

In this paper an iteration scheme is presented which differs from the one used in [2]. The scheme is based upon the almost parabolic behaviour of the Navier–Stokes equations and it leads to much faster convergence than could be obtained with the method from [2]. Especially for large and small values of Re very fast convergence is obtained.

For the parabolic cylinder an analytic expression could be found for the total drag acting upon the parabola (see Botta, Dijkstra and Veldman [2]). For the paraboloid of revolution also such an expression can be derived. The total drag then is given by an asymptotic series valid far downstream. The first two terms of this series are generated by the subtracted behaviour at infinity, so that the most important term to which the numerically calculated quantities give a contribution is the third term of the series. The analytic value of this third term has been used as a check for the numerical results and good agreement is obtained.

By the time this paper was finished a paper by Davis and Werle [11] was published which also treats flow past a paraboloid. Davis and Werle solve the Navier–Stokes equations by means of an implicit alternating direction method. They solve parabolic boundary layer type equations in one iteration step, and correct for the elliptic behaviour of the Navier–Stokes equations in the next iteration step. The use of boundary layer techniques in the iteration process leads to a convergence of the numerical calculations which is comparable with ours. For large values of the coordinates their solution is believed to be less accurate, since Davis and Werle do not subtract the behaviour at infinity. Moreover their transformation of the infinite region of interest is not optimal. Because Davis and Werle present diagrams but no tables, only a rough graphical comparison with their results can be made. Good agreement is indicated.

2. BASIC EQUATIONS

The Navier–Stokes equations for an incompressible viscous fluid can be written as

$$\begin{aligned} &\operatorname{div} \mathbf{q} = 0 \\ &\tfrac{1}{2} \operatorname{grad} q^2 - \mathbf{q} \times \operatorname{rot} \mathbf{q} = -\frac{1}{\rho} \operatorname{grad} p - \nu \operatorname{rot} \operatorname{rot} \mathbf{q} \end{aligned} \tag{2.1}$$

where $\mathbf{q}$ denotes the velocity, p the pressure, ρ the density and ν the kinematic viscosity. The pressure can be eliminated from the second equation of (2.1) by taking its rot. When $\boldsymbol{\omega} = \operatorname{rot} \mathbf{q}$ we can write

$$\begin{aligned} &\operatorname{div} \mathbf{q} = 0 \\ &\operatorname{rot}(\mathbf{q} \times \boldsymbol{\omega}) = \nu \operatorname{rot} \operatorname{rot} \boldsymbol{\omega} \end{aligned} \tag{2.2}$$

Since we want to study axisymmetric flow, we introduce cylindrical polar coordinates (x, r, θ). Let the paraboloid be given by $r^2 = 4a(x + a)$, where a is half the nose-radius of the paraboloid. The oncoming flow is supposed to be uniform with velocity U_0 and parallel to the x-axis. Now the boundary conditions to equation (2.2) are

$$\begin{aligned} &\mathbf{q} = 0 \qquad \text{at the paraboloid,} \\ &\mathbf{q} \to U_0 \mathbf{i}_x \qquad \text{for } x \to -\infty. \end{aligned} \tag{2.3}$$

To satisfy the first equation of (2.2) we introduce a streamfunction ψ according to

$$u = r^{-1} \frac{\partial \psi}{\partial r} \quad \text{and} \quad v = -r^{-1} \frac{\partial \psi}{\partial x},$$

where u and v are the velocity components in x- and r-directions. Next we define nondimensional variables in the following way

$$\begin{aligned} x + ir &= \nu(\sqrt{\xi} + i\sqrt{\eta})^2/U_0, \\ \psi &= 2\nu^2\Psi/U_0. \end{aligned} \tag{2.4}$$

Now the paraboloid is given by

$$\eta = Re = U_0 a/\nu \tag{2.5}$$

where Re is the Reynolds number based upon the characteristic length a.

In non-viscous plane flow, the vorticity ω remains constant along streamlines. The nondimensional quantity which has this property in axisymmetric flow is given by

$$G = \frac{2\nu^2}{U_0^3}\frac{\omega}{r}. \tag{2.6}$$

With these new variables the Navier–Stokes equations (2.2) become

$$\xi\frac{\partial^2 G}{\partial \xi^2} + 2\frac{\partial G}{\partial \xi} + \eta\frac{\partial^2 G}{\partial \eta^2} + 2\frac{\partial G}{\partial \eta} = \frac{\partial G}{\partial \xi}\frac{\partial \Psi}{\partial \eta} - \frac{\partial G}{\partial \eta}\frac{\partial \Psi}{\partial \xi} \tag{2.7a}$$

$$\xi\frac{\partial^2 \Psi}{\partial \xi^2} + \eta\frac{\partial^2 \Psi}{\partial \eta^2} = -\xi\eta(\xi + \eta)G. \tag{2.7b}$$

When Re is very small, G has an almost singular behaviour near the nose of the paraboloid. This can be seen as follows:

From symmetry we have $\Psi(0, \eta) = \Psi(\xi, Re) = 0$ and the no-slip condition yields $\partial\Psi/\partial\eta(\xi, Re) = 0$. Therefore a Taylor series for the streamfunction near the nose of the paraboloid must begin with $\Psi \sim A\xi(\eta - Re)^2$, where A is some constant which is unlikely to be zero. From equation (2.7b) we find that the corresponding term for G is given by $G \sim -2A(\xi + Re)^{-1}$, and this is a singular term when $Re = 0$. Note the analogy with the vorticity in plane flow (see [1] and [2]).

Furthermore, when $\xi = 0$ in the right hand side of (2.6) both numerator and denominator are zero, which leads to an undefined value for G. We therefore introduce a new variable

$$L = -\xi(\xi + \eta)G. \tag{2.8}$$

The factor $(\xi + \eta)$ is used to remove the singularity and the factor ξ makes L vanish on $\xi = 0$. Equation (2.7) can now be expressed as

$$\xi\frac{\partial^2 L}{\partial \xi^2} + \eta\frac{\partial^2 L}{\partial \eta^2} - \frac{2\xi}{\xi + \eta}\left(\frac{\partial L}{\partial \xi} - \frac{\partial L}{\partial \eta}\right) = \frac{\partial L}{\partial \xi}\frac{\partial \Psi}{\partial \eta} - \frac{\partial L}{\partial \eta}\frac{\partial \Psi}{\partial \xi} + \frac{L}{\xi + \eta}\left\{\frac{\partial \Psi}{\partial \xi} - \left(2 + \frac{\eta}{\xi}\right)\frac{\partial \Psi}{\partial \eta}\right\} \tag{2.9a}$$

$$\xi\frac{\partial^2 \Psi}{\partial \xi^2} + \eta\frac{\partial^2 \Psi}{\partial \eta^2} = \eta L \tag{2.9b}$$

with boundary conditions

$$\xi = 0: \quad \Psi = L = 0 \tag{2.10a}$$

$$\eta = Re: \quad \Psi = \frac{\partial \Psi}{\partial \eta} = 0 \tag{2.10b}$$

$$\xi \text{ and/or } \eta \to \infty: \quad \Psi \sim \xi f(\eta) + \frac{\xi}{\xi+\eta} f_0(\eta), \quad L \sim \xi f''(\eta) + \frac{\xi}{\xi+\eta} f_0''(\eta). \tag{2.10c}$$

The conditions (2.10c) will be discussed in the next section.

The quantities Ψ and L are unbounded at infinity. We therefore introduce the departures of the solution from the behaviour at infinity

$$\Psi_1 = \Psi - \xi f(\eta) - \xi(\xi+\eta)^{-1} f_0(\eta) \tag{2.11a}$$

$$L_1 = L - \xi f''(\eta) - \xi(\xi+\eta)^{-1} f_0''(\eta) + 2\xi(\xi+\eta)^{-2} f_0'(\eta). \tag{2.11b}$$

The last term in (2.11b) is an extra term, inserted to keep equation (2.9b) in its simplest form after substitution. This substitution changes equations (2.9) into

$$\begin{aligned} \xi\left(\frac{\partial^2 L_1}{\partial \xi^2} + C_1\right) + \eta\left(\frac{\partial^2 L_1}{\partial \eta^2} + C_2\right) - \frac{2\xi}{\xi+\eta}\left(\frac{\partial L_1}{\partial \xi} + C_3 - \frac{\partial L_1}{\partial \eta} - C_4\right) \\ = \left(\frac{\partial L_1}{\partial \xi} + C_3\right)\left(\frac{\partial \Psi_1}{\partial \eta} + C_6\right) - \left(\frac{\partial L_1}{\partial \eta} + C_4\right)\left(\frac{\partial \Psi_1}{\partial \xi} + C_5\right) \\ + \frac{L_1 + C_7}{\xi+\eta}\left\{\frac{\partial \Psi_1}{\partial \xi} + C_5 - \left(2 + \frac{\eta}{\xi}\right)\left(\frac{\partial \Psi_1}{\partial \eta} + C_6\right)\right\} \\ \xi \frac{\partial^2 \Psi_1}{\partial \xi^2} + \eta \frac{\partial^2 \Psi_1}{\partial \eta^2} = \eta L_1. \end{aligned} \tag{2.12}$$

The boundary conditions are now completely homogeneous

$$\begin{aligned} &\xi = 0: \quad \Psi_1 = L_1 = 0, \\ &\eta = Re: \quad \Psi_1 = \frac{\partial \Psi_1}{\partial \eta} = 0, \\ &\xi \to \infty: \quad \Psi_1 \to 0, \quad L_1 \to 0 \\ &\eta \to \infty: \quad \Psi_1 \to 0, \quad L_1 \to 0 \text{ (exponentially)} \end{aligned} \tag{2.13}$$

To derive these conditions use has been made of results from the next section.

That the vorticity decays exponentially as $\eta \to \infty$ has been proved for flow past finite bodies by Clark [12]. For flow past infinite bodies no full mathematical proof is available until now.

The quantities C_i, $i = 1, \ldots, 7$ appearing in equations (2.12) can be easily expressed in the subtracted functions f and f_0.

3. THE ASYMPTOTIC BEHAVIOUR FAR FROM THE NOSE

Miller [9] has given a very detailed investigation on the behaviour of the solution for large values of the coordinates. In this section we will present his most important results.

The method used by Miller to find the behaviour at infinity is based upon the matching of two asymptotic expansions. One is valid far from the paraboloid surface (ξ, $\eta \to \infty$) where we have potential flow. The other one is valid near the paraboloid surface ($\xi \to \infty$, η finite) where the full Navier–Stokes equations must be used. This last region we call boundary layer.

First consider the potential region. In the meridian plane we define nondimensional polar coordinates (ρ, ϕ) by

$$U_0 x/\nu = \rho \cos \phi, \qquad U_0 r/\nu = \rho \sin \phi.$$

In the potential region L is exponentially small, hence equation (2.9b) reduces to

$$\xi \frac{\partial^2 \Psi}{\partial \xi^2} + \eta \frac{\partial^2 \Psi}{\partial \eta^2} = 0.$$

Written in polar coordinates we have

$$\rho^2 \frac{\partial^2 \Psi}{\partial \rho^2} + (1 - \mu^2) \frac{\partial^2 \Psi}{\partial \mu^2} = 0 \tag{3.1}$$

where $\mu = \cos \phi$. The relation between (ρ, μ) and (ξ, η) is given by $\rho = \xi + \eta$ and $\mu = (\xi - \eta)/(\xi + \eta)$.

To start with, we let the asymptotic series of Ψ for large values of ρ consist of integer powers of ρ. Together with the condition $\Psi = 0$ as $\xi = 0$ $(\phi = \pi)$ equation (3.1) has exactly one solution for each power of ρ. The beginning of the series thus becomes

$$\Psi = A_2 \rho^2 (1 - \mu^2) + A_1 \rho (1 + \mu) + A_0 (1 + \mu) + A_{-1} \left(\frac{1 - \mu^2}{\rho} \right) + \cdots \tag{3.2}$$

The coefficients A_i must be determined by matching. The first term must match the oncoming flow $\Psi = \xi\eta$, which results in $A_2 = \frac{1}{4}$. Equation (3.2) re-expanded for large ξ and finite η gives

$$\Psi = \xi\eta \quad 2A_1 \xi + 2A_0 + (-2A_0 \eta) \frac{1}{\xi} + \cdots \tag{3.3}$$

In the boundary layer region (η finite) we assume the asymptotic expansion to be

$$\Psi = \xi f(\eta) + f_0(\eta) + \frac{1}{\xi} f_1(\eta) + \cdots \tag{3.4}$$

Substituting this in equation (2.9) and evaluating terms with equal powers of ξ we derive equations for the unknown functions f and f_i, $i = 0, 1, \ldots$.

The first equation is

$$\eta f''' + 2f''' + f'f'' + ff''' = 0$$

which can be integrated once, obtaining

$$\eta f''' + f'' + ff'' = 0. \tag{3.5a}$$

The integration constant vanishes because for large η all second and higher derivatives of f must be exponentially small because of the exponential decay of vorticity. Boundary conditions are given by

$$f(Re) = f'(Re) = 0 \quad \text{and} \quad f'(\infty) = 1. \tag{3.5b}$$

The first two follow from (2.10b). The third one comes from the matching of the first terms of (3.3) and (3.4). Equation (3.5) is used to calculate f. This has been done by means of a simple shooting method. Some numerical values concerning f are presented by Veldman [13]. For large η the behaviour of f is

$$f \sim \eta - \beta + \text{exp. small terms.} \tag{3.6}$$

Here β is a constant which follows from the numerical computations. The second term of (3.3) can now be matched which results in $A_1 = -\frac{1}{2}\beta$.

The equation for f_0 can be written as

$$\eta f_0''' + (f+2)f_0''' + 2f'f_0'' + f''f_0' = \eta f'f'' - ff''. \tag{3.7a}$$

The boundary conditions are

$$f_0(Re) = f_0'(Re) = 0 \quad \text{and} \quad f_0'(\infty) = 0. \tag{3.7b}$$

Again the first two follow from (2.10b) and the third one from matching with (3.3). Also the second and higher derivatives of f_0 must decay exponentially. Since $f_0'(\infty) = 0$, f_0 approaches a constant when $\eta \to \infty$. This constant determines A_0 in (3.3), viz. $A_0 = \frac{1}{2}f_0(\infty)$. To calculate f_0 numerically equation (3.7) can be integrated twice resulting in

$$\eta f_0'' + ff_0' = \tfrac{1}{2}(\eta ff' - f^2 + \eta^2 f'' + C_1\eta + C_2). \tag{3.8}$$

C_1 and C_2 are integration constants which can be evaluated by noting that the left hand side of equation (3.8) tends to zero as $\eta \to \infty$, and so must the right hand side. When we use the behaviour of f given by (3.6) we obtain by putting the right hand side of (3.8) equal to zero, $C_1 = -\beta$ and $C_2 = \beta^2$. Equation (3.8) can now be integrated directly since two boundary conditions on the inner boundary are known. Some important values concerning f_0 are

$$f_0''(Re) = \tfrac{1}{2}\{\beta^2 Re^{-1} - \beta + Ref''(Re)\} \quad \text{and} \quad f_0'''(Re) = -\tfrac{1}{2}\beta^2 Re^{-2}. \tag{3.9}$$

The values of $f_0(\infty)$ can also be found in Veldman [13].

Apart from the terms with integral powers of ρ equation (3.1) also has solutions with non-integer powers of ρ. Miller has pointed out that the leading term of such a solution of order ρ^{-k}, when expanded for large ξ, has the form $A_k\xi^{-k}$. For a corresponding term $\xi^{-k}f_k(\eta)$ in (3.4) this means that an outer boundary condition $f_k'(\infty) = 0$ exists. The other conditions are as always $f_k(Re) = f_k'(Re) = 0$ and $f_k''(\infty) = 0$ exp. The function $f_k(\eta)$ satisfies the homogeneous equation

$$\eta f_k''' + (f+2)f_k''' + (k+2)f'f_k'' + f''f_k' - kf'''f_k = 0. \tag{3.10}$$

It appears that for some values of k this homogeneous equation together with the homogeneous boundary conditions has a non-trivial solution. These values of k are called eigenvalues. Calculation of the eigenvalues shows that the smallest value k_1 lies between 0 and 1 for all Re. Therefore this creates in (3.4) a term of order ξ^{-k_1} which comes directly after the term $f_0(\eta)$. For details on the calculation of the first four eigenvalues see Veldman [13]. In Table 1 we present k_1 for several values of Re. In the appendix we prove that all eigenvalues tend to integers as Re approaches zero.

Table 1. The smallest eigenvalue k_1

Re	k_1	Re	k_1
10^{-5}	0·088	10	0·686
10^{-3}	0·142	10^3	0·950
10^{-1}	0·295	10^5	0·995

We are now able to derive boundary conditions (2.10c). When we write (3.2) in terms of ξ and η we find after using the matching results for A_2, A_1 and A_0

$$\Psi \sim \xi(\eta - \beta) + \frac{\xi}{\xi + \eta} f_0(\infty). \tag{3.11}$$

Combining this with (3.4) we can form an expansion valid in both potential region and boundary layer when we write

$$\Psi \sim \xi f(\eta) + \frac{\xi}{\xi + \eta} f_0(\eta). \tag{3.12}$$

From this expansion together with (2.9b) boundary conditions (2.10c) are found.

We have also seen that the most important term after the two terms in (3.12) is of the order ρ^{-k_1}. This then is the order of the variables Ψ_1 and L_1 defined in (2.11). Since the smallest eigenvalue is positive we conclude that for large values of the coordinates the functions Ψ_1 and L_1 tend to zero, thus yielding homogeneous boundary conditions as was stated in section 2.

4. BEHAVIOUR OF THE SOLUTION FOR $Re \to \infty$ AND $Re \to 0$

If $Re \to \infty$, i.e. $\nu \to 0$ transformation (2.4) loses sense and it should be replaced by

$$x + ir = a(\sqrt{\lambda} + i\sqrt{\mu})^2, \qquad \psi = 2a^2 U_0 \psi_b \quad \text{and} \quad G = Re^{-2} G_b. \tag{4.1}$$

The paraboloid can now be expressed by $\mu = 1$. In these new variables the Navier-Stokes equations are given by

$$\begin{aligned} \lambda \frac{\partial^2 G_b}{\partial \lambda^2} + 2\frac{\partial G_b}{\partial \lambda} + \mu \frac{\partial^2 G_b}{\partial \mu^2} + 2\frac{\partial G_b}{\partial \mu} &= Re\left(\frac{\partial G_b}{\partial \lambda}\frac{\partial \psi_b}{\partial \mu} - \frac{\partial G_b}{\partial \mu}\frac{\partial \psi_b}{\partial \lambda}\right) \\ \lambda \frac{\partial^2 \psi_b}{\partial \lambda^2} + \mu \frac{\partial^2 \psi_b}{\partial \mu^2} &= -\lambda\mu(\lambda + \mu) G_b. \end{aligned} \tag{4.2}$$

To describe the flow pattern properly for large Re we must use a stretching transformation

$$\mu - 1 = Re^{-1/2}\mu_b, \qquad \psi_b = Re^{-1/2}\Psi_b. \tag{4.3}$$

Substitution of the transformation (4.3) into equations (4.2) yields in the limit $Re \to \infty$ a fourth order differential equation for the streamfunction Ψ_b which can be integrated once with respect to μ_b. The result then becomes

$$\lambda(\lambda + 1)\left\{\frac{\partial^3 \Psi_b}{\partial \mu_b^3} + \frac{\partial^2 \Psi_b}{\partial \mu_b^2}\frac{\partial \Psi_b}{\partial \lambda} - \frac{\partial^2 \Psi_b}{\partial \mu_b \partial \lambda}\frac{\partial \Psi_b}{\partial \mu_b}\right\} + (\lambda + \tfrac{1}{2})\left(\frac{\partial \Psi_b}{\partial \mu_b}\right)^2 = -\tfrac{1}{2}\lambda^2 \tag{4.4}$$

where the right hand side has been determined by matching Ψ_b for $\mu_b \to \infty$ with the outer potential flow given by $\lambda\mu_b$. The boundary conditions are

$$\begin{aligned} &\Psi_b(0, \mu_b) = 0, \\ &\Psi_b(\lambda, 0) = \frac{\partial \Psi_b}{\partial \mu_b}(\lambda, 0) = 0, \\ &\frac{\partial \Psi_b}{\partial \mu_b}(\lambda, \mu_b) \to \lambda \quad \text{for } \mu_b \to \infty. \end{aligned} \tag{4.5}$$

For large values of λ the solution of equation (4.4) can be written as $\Psi_b = \lambda F(\mu_b)$ where F satisfies

$$F''' + FF'' = 0, \qquad F(0) = F'(0) = 0, \qquad F'(\infty) = 1. \tag{4.6}$$

Thus we see that F is the well-known Blasius function.

For small values of λ the solution can be written as $\Psi_b = \lambda G(\mu_b)$, with G satisfying

$$G''' + GG'' - \tfrac{1}{2}(G'^2 - 1) = 0, \qquad G(0) = G'(0) = 0, \qquad G'(\infty) = 1. \tag{4.7}$$

This is a special case of the Falkner–Skan equation.

For all values of λ equation (4.4) has been solved by Smith and Clutter [3] and by Davis [4].

From these solutions we infer that the variables λ, μ_b and Ψ_b are the proper ones to work with when we deal with large values of Re. The relation between these variables and the ones introduced in section 2 can be found from (2.4), (4.1) and (4.3) resulting in

$$\xi = Re\lambda, \qquad \eta - Re = Re^{1/2}\mu_b, \qquad \Psi = Re^{3/2}\Psi_b, \qquad L = Re^{1/2}L_b, \tag{4.8}$$

where L_b is defined by $L_b = \partial^2\Psi_b/\partial\mu_b{}^2$, which is the boundary layer form of (2.9b).

For small values of Re there is a neighbourhood of the paraboloid where we have Stokes flow. The velocity in this region is so small that we may neglect the non-linear terms in the Navier–Stokes equations. It is appropriate to introduce Stokes variables according to

$$x + ir = a(\sqrt{\lambda} + i\sqrt{\mu})^2, \qquad \psi = 2a^2U_0\psi_s, \qquad G = Re^{-2}G_s. \tag{4.9}$$

Hence the Navier–Stokes equations become

$$\begin{aligned} \lambda\frac{\partial^2 G_s}{\partial\lambda^2} + 2\frac{\partial G_s}{\partial\lambda} + \mu\frac{\partial^2 G_s}{\partial\mu^2} + 2\frac{\partial G_s}{\partial\mu} &= 0 \\ \lambda\frac{\partial^2\psi_s}{\partial\lambda^2} + \mu\frac{\partial^2\psi_s}{\partial\mu^2} &= -\lambda\mu(\lambda + \mu)G_s \end{aligned} \tag{4.10}$$

Boundary conditions are

$$\psi_s(0, \mu) = \psi_s(\lambda, 1) = \frac{\partial\psi_s}{\partial\mu}(\lambda, 1) = 0.$$

The solution of equation (4.10) is given by

$$\psi_s = C\lambda(\mu\log\mu - \mu + 1), \tag{4.11}$$

where C has to be determined from an outer boundary condition. This condition can be found by matching (4.11) with an outer solution, for instance the Oseen solution. The leading term of such an outer solution is always $\xi\eta$. When we write (4.11) in outer variables ξ, η and Ψ the most important term for small Re is given by $\Psi \sim -C\xi\eta\log Re$. This must match the outer flow, resulting in

$$C = -(\log Re)^{-1}. \tag{4.12}$$

We now observe the existence of three regions:

(i) The Stokes region where the Stokes approximation is valid. In this region $\mu = O(1)$ which means $\eta = O(Re)$.

(ii) A transition region where one might use the Oseen approximation. Here $\eta = O(1)$.

(iii) Far away from the surface of the paraboloid where the vorticity has become zero we have the potential region.

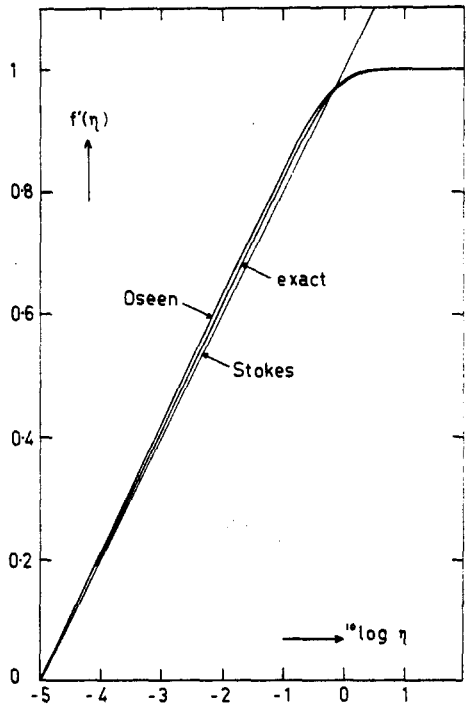

Fig. 1. Downstream velocity profiles in Stokes approximation, Oseen approximation and exact for $Re = 10^{-5}$.

These regions are visible in Fig. 1 where the downstream velocity profile $f'(\eta)$ is drawn for a Reynolds number of 10^{-5}. We see that in the Stokes region where $\eta = O(10^{-5})$ there is an important variation in $f'(\eta)$. Therefore we must take this Stokes region into account if we want to solve the Navier–Stokes equations numerically.

Also shown in Fig. 1 are the Stokes approximation and the Oseen approximation for the velocity profile. The Stokes value can be obtained by combination of (3.4) and (4.11) which results in

$$f_S'(\eta) = 1 - \log \eta / \log Re.$$

The Oseen value is found most simply by linearization of equation (3.5) around the oncoming flow. We thus write

$$\eta f''' + (\eta + 1) f'' = 0, \qquad f(Re) = f'(Re) = 0, \qquad f'(\infty) = 1. \tag{4.13}$$

From the solution of this equation we derive

$$f_{0s}'(\eta) = 1 - E_1(\eta)/E_1(Re), \quad \text{where} \quad E_1(x) = \int_x^\infty e^{-t} t^{-1}\, dt.$$

The thickness of the boundary layer is in Fig. 1 seen to be of the order $\eta = O(10)$. Hence the boundary layer of a thin paraboloid is much thicker than the paraboloid itself. But there is only a limited region $[\eta = o(1)]$ in the boundary layer where the flow differs significantly from the oncoming flow. In that region (4.13) may be approximated by

$$\eta f''' + f'' = 0 \tag{4.14}$$

in which the non-linear term is neglected. There is almost no difference in that region between

(i) the solution of (4.14), which is the Stokes solution,
(ii) the solution of (4.13), which is the Oseen solution and
(iii) the solution of (3.5), which is the exact solution.

5. REFORMULATION OF THE PROBLEM

In the preceding section we have seen that the variables introduced in section 2, i.e. ξ, η, Ψ and L, are not the best ones to use for all values of Re. For large Re the variables λ, μ_b, Ψ_b and L_b are the proper ones. For small Re we have a Stokes region where Stokes variables should be used and a transition region where the variables from section 2 seem to be the best ones in order to keep all used quantities of order unity.

To combine these cases we introduce the following transformation

$$\xi = A^2\hat{\xi}, \qquad \eta - Re = A\hat{\eta} \tag{5.1}$$

with

$$A = 1 + Re^{1/2}.$$

For large Re we see that $\hat{\xi}$ and $\hat{\eta}$ tend to the boundary layer variables λ and μ_b. For small Re we have chosen $\hat{\xi}$ to be approximately equal to ξ. Although $\hat{\xi}$ now is no Stokes variable it appeared from the numerical calculations that $\hat{\xi}$ was the best variable to use. In the η-direction we must accept a small difficulty, namely that $\hat{\eta}$ is $O(Re)$ in the Stokes region and $O(1)$ in the transition region.

The corresponding new variables for streamfunction and vorticity are given by

$$\Psi = A^3\hat{\Psi} \quad \text{and} \quad L = A\hat{L}. \tag{5.2a}$$

Instead of Ψ_1 and L_1 defined in (2.11) we use

$$\hat{\Psi}_1 = A^{-3}\Psi_1 \quad \text{and} \quad \hat{L}_1 = A^{-1}L_1. \tag{5.2b}$$

Another difficulty arises from the infinite extent of the region of interest when we solve equations (2.12) numerically. To overcome this difficulty we follow the method used by van de Vooren and Dijkstra [1] by transforming the infinite region in the $(\hat{\xi}, \hat{\eta})$-plane to a finite rectangle in the (σ, τ)-plane. As finite region we take the square

$$0 \leqq \sigma \leqq 1, \qquad 0 \leqq \tau \leqq 1. \tag{5.3}$$

In $\hat{\xi}$-direction we base the transformation upon the behaviour of $\hat{\Psi}_1$ and $\hat{L}_1$ for $\hat{\xi} \to \infty$. In section 3 we have seen that this behaviour is like ξ^{-k_1}, where k_1 is the smallest eigenvalue. We choose the transformation such that the derivatives of the solution with respect to σ are of the order unity for large $\hat{\xi}$. The transformation used is given by

$$\sigma = 1 - (E\hat{\xi} + 1)^{-z_1}. \tag{5.4}$$

The constant E appearing is chosen such that the maximum of $|\hat{L}_1|$ lies in the middle of the σ-interval. The best way to choose z_1 is to take it equal to k_1. From the numerical calculation it appeared that this choice was not absolutely necessary, since any choice of z_1 not too far from k_1 gave satisfactory results. In the final calculations we have taken $z_1 < k_1$ for a reason mentioned by Veldman [13]. For values of $Re > 1$ we have used $z_1 = \frac{1}{2}$ and $E = 2$ (see Table 1 for the eigenvalues). For each of the other values of Re different z_1 and E were chosen.

In $\hat{\eta}$-direction the transformation is taken such that the boundary layer region is transformed to $0 \leqq \tau \leqq \frac{1}{2}$ and the potential region to $\frac{1}{2} \leqq \tau \leqq 1$. For $Re > 1$ the simple expression

$$\hat{\eta} = D \frac{\tau}{1-\tau} \tag{5.5}$$

gives excellent results. The constant D is evaluated such that the edge of the boundary layer is transformed to $\tau = \frac{1}{2}$. This edge is defined as the value of $\hat{\eta}$ where $\hat{L}_1$ becomes $O(10^{-7})$ compared to $O(10^{-1})$ at the paraboloid surface. Also at this value of $\hat{\eta}$ we have $1 - f'(\eta) = O(10^{-8})$.

For values of $Re \leqq 1$ transformation (5.5) cannot be used. The appearance of the Stokes region becomes important and (5.5) then gives too few points in this region. Now another transformation is used which gives more points near the paraboloid surface

$$\hat{\eta} = C_1 \frac{\tau^{z_2}}{1-\tau} + C_2 \tau, \qquad z_2 > 1 \tag{5.6}$$

The term $C_2 \tau$ is needed because $d\hat{\eta}/d\tau$ must be unequal to zero when $\tau = 0$. The exponent z_2 and the constants C_1 and C_2 are chosen such that we have a reasonable spreading of the Stokes region and the transition region over $0 \leqq \tau \leqq \frac{1}{2}$. A good choice for most of the Reynolds numbers is $C_1 = 200$ and $C_2 = 5Re$. The value of z_2 varies from 3 to 7 for Re between 1 and 10^{-5}.

After the transformation to (σ, τ) and the substitution of (5.2b) the Navier–Stokes equations (2.12) are written as

$$\begin{aligned}
&\frac{\partial^2 \hat{L}_1}{\partial \sigma^2} \xi \sigma'^2 + \frac{\partial^2 \hat{L}_1}{\partial \tau^2} \eta \tau'^2 + \frac{\partial \hat{L}_1}{\partial \tau} \left\{ \eta \tau'' + A^2 \tau' \left(\frac{2A\hat{\xi}}{\xi + \eta} + \frac{\partial \hat{\Psi}_1}{\partial \sigma} \sigma' + \hat{C}_5 \right) \right\} \\
&\quad - \hat{L}_1 \frac{A^2}{\xi + \eta} \left\{ A \left(\frac{\partial \hat{\Psi}_1}{\partial \sigma} \sigma' + \hat{C}_5 \right) - \left(2A^2 + \frac{\eta}{\hat{\xi}} \right) \left(\frac{\partial \hat{\Psi}_1}{\partial \tau} \tau' + \hat{C}_6 \right) \right\} \\
&\quad - \frac{\partial \hat{\Psi}_1}{\partial \tau} A^2 \tau' \left\{ \frac{\partial \hat{L}_1}{\partial \sigma} \sigma' + \hat{C}_3 - \frac{\hat{C}_7}{\xi + \eta} \left(2A^2 + \frac{\eta}{\hat{\xi}} \right) \right\} \\
&\quad = \frac{\partial \hat{L}_1}{\partial \sigma} \left\{ -\hat{\xi} \sigma'' + A^2 \sigma' \left(\frac{2\hat{\xi}}{\xi + \eta} + \hat{C}_6 \right) \right\} + \frac{\partial \hat{\Psi}_1}{\partial \sigma} A^2 \sigma' \left\{ \frac{A\hat{C}_7}{\xi + \eta} - \hat{C}_4 \right\} \\
&\quad\quad - \hat{C}_1 \hat{\xi} - \hat{C}_2 \eta + A^2 \left[\hat{C}_3 \frac{2\hat{\xi}}{\xi + \eta} - \hat{C}_4 \frac{2A\hat{\xi}}{\xi + \eta} + \hat{C}_3 \hat{C}_6 - \hat{C}_4 \hat{C}_5 \right. \\
&\quad\quad \left. + \frac{\hat{C}_7}{\xi + \eta} \left\{ A\hat{C}_5 - \left(2A^2 + \frac{\eta}{\hat{\xi}} \right) \hat{C}_6 \right\} \right]
\end{aligned} \tag{5.7a}$$

$$\frac{\partial^2 \hat{\Psi}_1}{\partial \sigma^2} \hat{\xi} \sigma'^2 + \frac{\partial^2 \hat{\Psi}_1}{\partial \tau^2} \eta \tau'^2 + \frac{\partial \hat{\Psi}_1}{\partial \tau} \eta \tau'' - \hat{L}_1 \eta = - \frac{\partial \hat{\Psi}_1}{\partial \sigma} \hat{\xi} \sigma'' \tag{5.7b}$$

In the potential region we may take $\hat{L}_1$ numerically equal to zero and from equations (2.12) there only remains

$$\frac{\partial^2 \hat{\Psi}_1}{\partial \sigma^2} \hat{\xi} \sigma'^2 + \frac{\partial^2 \hat{\Psi}_1}{\partial \tau^2} \eta \tau'^2 + \frac{\partial \hat{\Psi}_1}{\partial \tau} \eta \tau'' = - \frac{\partial \hat{\Psi}_1}{\partial \sigma} \hat{\xi} \sigma'' \tag{5.7c}$$

The boundary conditions are given by

$$\begin{aligned} \sigma = 0: &\quad \hat{\Psi}_1 = \hat{L}_1 = 0, \\ \tau = 0: &\quad \hat{\Psi}_1 = \partial\hat{\Psi}_1/\partial\tau = 0, \\ \sigma = 1: &\quad \hat{\Psi}_1 = \hat{L}_1 = 0, \\ \tau = 1: &\quad \hat{\Psi}_1 = 0, \\ \tau = \tfrac{1}{2} + \Delta\tau: &\quad \hat{L}_1 = 0. \end{aligned} \tag{5.8}$$

The boundary condition for $\hat{L}_1$ at infinity ($\hat{\eta} \to \infty$) can be taken at the edge of the boundary layer. It has been taken at $\tau = \frac{1}{2} + \Delta\tau$ where $\Delta\tau$ is the meshsize in τ-direction.

6. THE NUMERICAL PROCEDURE

Equations (5.7) have been replaced by a system of difference equations based on a net of which the netpoints have coordinates

$$\begin{aligned} &\sigma = ph \quad (p = 0, 1, \ldots, N;\ Nh = 1), \\ &\tau = qk \quad (q = 0, 1, \ldots, 2M;\ 2Mk = 1). \end{aligned} \tag{6.1}$$

Derivatives have been replaced by central difference expressions. Then equations (5.7) can be written in the following form

$$\begin{aligned} a_{11}\hat{L}_{1n,m-1} + b_{11}\hat{L}_{1n,m} + c_{11}\hat{L}_{1n,m+1} + a_{12}\hat{\Psi}_{1n,m-1} + b_{12}\hat{\Psi}_{1n,m} + c_{12}\hat{\Psi}_{1n,m+1} \\ = d_{11}\hat{L}_{1n-1,m} + e_{11}\hat{L}_{1n+1,m} + d_{12}\hat{\Psi}_{1n-1,m} + e_{12}\hat{\Psi}_{1n+1,m} + f_1 \end{aligned} \tag{6.2a}$$

$$a_{22}\hat{\Psi}_{1n,m-1} + b_{22}\hat{\Psi}_{1n,m} + c_{22}\hat{\Psi}_{1n,m+1} + b_{21}\hat{L}_{1n,m} = d_{22}\hat{\Psi}_{1n-1,m}e_{22} + \hat{\Psi}_{1n+1,m} \tag{6.2b}$$

This form is valid in the boundary layer $m = 1, \ldots, M$. In the potential region it simplifies to

$$a\hat{\Psi}_{1n,m-1} + b\hat{\Psi}_{1n,m} + c\hat{\Psi}_{1n,m+1} = d\hat{\Psi}_{1n-1,m} + e\hat{\Psi}_{1n+1,m} \tag{6.2c}$$

with

$$m = M + 1, \ldots, 2M - 1.$$

In these expressions $\hat{L}_{1n,m-1}$ denotes $\hat{L}_1(nh, (m-1)k)$ and analogously for the other terms.

The coefficients $a_{11}, b_{11}, \ldots$ are found by writing out (5.7). The term $b_{12}\hat{\Psi}_{1n,m}$ will be introduced in the sequel. How the non-linear terms in (5.7a) are treated is suggested by the form in which this equation is written. For instance in the term

$$\frac{\partial\hat{L}_1}{\partial\tau}\left\{\eta\tau'' + A^2\tau'\left(2A\hat{\xi}(\xi+\eta)^{-1} + \frac{\partial\hat{\Psi}_1}{\partial\sigma}\sigma' + \hat{C}_5\right)\right\}$$

we regard the expression between parentheses including $\partial\hat{\Psi}_1/\partial\sigma$ as a coefficient and calculate it from previously found values of $\hat{\Psi}_1$. In (6.2a) it then gives a contribution to a_{11} and c_{11}.

The boundary conditions to equations (6.2) are found directly from (5.8) except for the condition $\partial\hat{\Psi}_1/\partial\tau(\sigma, 0) = 0$ which must be written in a different form. To do so we combine it with equation (5.7b) which at the parabola surface reduces to $\tau'^2(\partial^2\hat{\Psi}_1/\partial\tau^2) = \hat{L}_1$. We then can derive that

$$\hat{L}_{1n,0} = \frac{8\hat{\Psi}_{1n,1} - \hat{\Psi}_{1n,2}}{2k^2}\tau'^2.$$

This form has also been used in [2].

After substitution of the boundary conditions, equations (6.2) have been solved using a line-iteration method along lines $\sigma =$ constant. The computations are started along the line $\sigma = h$ and proceed in the direction of increasing σ. The unknowns $\hat{L}_1(\sigma, \tau)$ and $\hat{\Psi}_1(\sigma, \tau)$ along a line $\sigma =$ constant, $\tau = qk$, $q = 1, 2, \ldots, 2M - 1$, are solved simultaneously from equations (6.2). For the values of $\hat{\Psi}_1$ and $\hat{L}_1$ appearing in the right hand side of (6.2) as well as in the coefficients in the left hand side we take the last calculated values.

In spite of the use of underrelaxation the iteration process described above appeared to be unstable for values of $Re > 1$. This instability was caused by the following phenomenon:

Regard a very simplified form of equation (5.7a)

$$\frac{1}{Re}\frac{\partial^2 L}{\partial \sigma^2} + \frac{\partial^2 L}{\partial \tau^2} - 2\frac{\partial L}{\partial \sigma} - 2\frac{\partial L}{\partial \tau} = 0 \tag{6.3}$$

Discretize this equation in the (σ, τ)-plane in the usual way with meshsizes h in both directions. Then we get

$$(Re^{-1} - h)L_{n+1,m} + (Re^{-1} + h)L_{n-1,m} + (1 - h)L_{n,m+1} + (1 + h)L_{n,m-1} - 2(1 + Re^{-1})L_{n,m} = 0$$

When this equation is solved by point iteration—Jacobi or Gauss–Seidel—the iteration process may be divergent if the matrix associated is not diagonally dominant. In fact diagonal dominance is a sufficient condition for convergence of linear systems. In our example diagonal dominance means

$$2|Re^{-1} + 1| \geqq |1 + h| + |1 - h| + |Re^{-1} + h| + |Re^{-1} - h|$$

When $h \leqq 1$ and $h \leqq Re^{-1}$ this condition is satisfied. But for large Re it is impossible in practice to choose $h \leqq Re^{-1}$ and hence diagonal dominance cannot be obtained in this way.

Greenspan [14] has suggested a method to retain diagonal dominance by using a backward difference expression for $\partial L/\partial \sigma$

$$\frac{\partial L}{\partial \sigma} = \frac{L_{n,m} - L_{n-1,m}}{h} \tag{6.4}$$

Using this method the iteration process becomes stable, but some accuracy is lost since central discretization of $\partial L/\partial \sigma$ has a smaller discretization error than the backward expression (6.4). To obtain central discretization accuracy Dennis and Chang [15] have suggested to add a correction term. They write

$$\frac{\partial L}{\partial \sigma} = \frac{L_{n,m} - L_{n-1,m}}{h} + \frac{L^{(a)}_{n+1,m} - 2L^{(a)}_{n,m} + L^{(a)}_{n-1,m}}{2h}. \tag{6.5}$$

The second part of (6.5) is the correction term and the superscript (a) indicates that it is calculated from previous values of L. In fact Dennis and Chang first solve (6.3) using (6.4) and, with this solution, they calculate the correction term and solve (6.3) again now using (6.5). They continue this process until overall convergence is obtained.

In the method used in this paper we calculate the correction term from the last calculated values, i.e. when we are doing the kth iteration step we write

$$\frac{\partial L}{\partial \sigma} = \frac{L^{(k)}_{n,m} - L^{(k)}_{n-1,m}}{h} + \frac{L^{(k-1)}_{n+1,m} - 2L^{(k-1)}_{n,m} + L^{(k)}_{n-1,m}}{2h}.$$

We can rewrite this as

$$\frac{\partial L}{\partial \sigma} = \frac{L^{(k-1)}_{n+1,m} - L^{(k)}_{n-1,m}}{2h} + \frac{L^{(k)}_{n,m} - L^{(k-1)}_{n,m}}{h}. \tag{6.6}$$

In this form we see that the usual central difference expression for $\partial L/\partial\sigma$ is used with a correction term which has the form of a time derivative (the iteration steps can be regarded as time steps). With expressions of the form (6.6) for $\partial \hat{L}_1/\partial\sigma$ and $\partial\hat{\Psi}_1/\partial\sigma$ substituted in (5.7) the resulting equations (6.2) were modified such that the iteration process became stable. A relaxation factor of 1 gave the fastest convergence.

For small Re a problem appeared concerning the subtracted terms in (2.11). The presence of a factor $(\xi + \eta)^{-1}$ in these subtracted terms means that at $\eta = Re$ these terms are considerably larger than Ψ and L. Since finally Ψ and L must be calculated from (2.11) after Ψ_1 and L_1 have been obtained, we are faced with loss of significant figures. This can be avoided by replacing $(\xi + \eta)^{-1}$ by $(\xi + \eta + 1)^{-1}$ which has the same behaviour for ξ and $\eta \to \infty$.

The initial solution for the iterative process has been taken identically zero, except for large Re where it appeared useful to start the iterations with the solution of equation (5.7) without the second order ξ-derivatives. To calculate this initial solution the method of Blottner and Flügge-Lotz [16] for the solution of the boundary layer equations has been used.

7. RESULTS

The flow field has been computed for the following values of the Reynolds number $Re = U_0 a/\nu$:

$$Re = 10^n, \qquad n = \text{integral values between } -5 \text{ and } 5$$

These values have been chosen such that they are representative of the entire range $0 < Re < \infty$. For each of these values, calculations have been performed with nets of the form $N \times 2M$ (see (6.1)). The used netsizes were 8×32, 16×64 and 32×128. The presented results are the ones obtained with the finest grid.

The iteration process was stopped when in the whole field the change in the variables $\hat{\Psi}_1$ and $\hat{L}_1$ due to 1 iteration step was nowhere more than a given tolerance. Convergence appeared to be the best for large and small Re. The slowest convergence occurred at $Re = 10$. To give an idea of the rate of convergence we have found that, at $Re = 10$, after 140 iterations the values of $\hat{L}_1$ in the whole field differed nowhere more than about 0.1 % from the finally-obtained values (after 287 iterations), when the finest grid was used. One iteration step with the 32×128 grid lasted 1.3 sec on a CDC Cyber 74-16 computer.

7.1. *Pressure*

At the paraboloid surface we have $\mathbf{q} = 0$ when the Navier–Stokes equations (2.1) can be written as

$$\frac{1}{\rho} \operatorname{grad} p = -\nu \operatorname{rot} \operatorname{rot} \mathbf{q}$$

When we combine this with (2.6) we can derive the following relations valid at the paraboloid surface

$$\frac{\partial P}{\partial \xi} = -\frac{\partial}{\partial \eta}(\eta G), \qquad \frac{\partial P}{\partial \eta} = \frac{\partial}{\partial \xi}(\xi G) \tag{7.1}$$

where P is the nondimensional pressure $P = (p - p_\infty)/\rho U_0{}^2$. Using (2.8) and (2.11) we obtain for the directional derivative of the pressure along the surface of the paraboloid the expression

$$\frac{\partial P}{\partial \xi} = \frac{\partial}{\partial \eta}\left\{\frac{\eta}{\xi+\eta}\left(\frac{L_1}{\xi} + f'' + \frac{1}{\xi+\eta} f_0'' - \frac{2}{(\xi+\eta)^2} f_0'\right)\right\} \quad \text{at } \eta = Re. \tag{7.2}$$

The pressure P can be found by integration of equation (7.2), starting at $\xi = \infty$ with a value of P equal to zero and integrating back along the surface.

The pressure P consists of two parts; one part is generated by the terms with f and f_0 and the other part is the contribution of the term involving L_1. These parts we denote by P_S and P_N respectively. Thus we have

$$P_S(\xi, Re) = \frac{Re}{\xi + Re}(f''(Re) - f_0'''(Re)) + \frac{Re - \xi}{(\xi + Re)^2} f_0''(Re) \tag{7.3a}$$

and

$$P_N(\xi, Re) = -\int_\xi^\infty \left\{\frac{L_1(\xi, Re)}{(\xi + Re)^2} + \frac{Re}{\xi(\xi + Re)} \frac{\partial L_1}{\partial \eta}(\xi, Re)\right\} d\xi. \tag{7.3b}$$

For large Re the pressure P approaches the pressure P_i which follows from inviscid theory. This inviscid pressure is given by

$$P_i = \frac{1}{2} \frac{Re}{\xi + Re}. \tag{7.4}$$

For a derivation of this result see Veldman [13]. He has also shown that

$$\lim_{Re \to \infty} P_N = P_i. \tag{7.5}$$

Results for P along the paraboloid surface are presented in Tables 2a and 2b and graphically in Fig. 2. A normalization factor $Re(1 + Re^{1/2})^{-2}$ has been used to keep the results of order unity for all Re. In Table 2a we have also tabulated the values of the inviscid pressure P_i at $Re = \infty$. These values can be found from (7.4) by letting Re go to infinity. Using (5.1) we find for this pressure $P_i(\xi) = \frac{1}{2}(\xi + 1)^{-1}$.

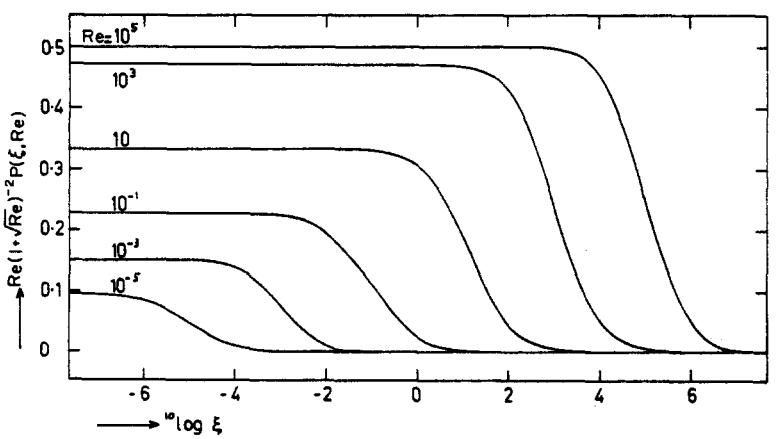

Fig. 2. Pressure at the paraboloid surface.

Table 2a. Pressure at the paraboloid

	$Re(1+Re^{1/2})^{-2}P(\xi, Re)$					
$\hat{\xi}$	$Re=10$	$Re=10^2$	$Re=10^3$	$Re=10^4$	$Re=10^5$	$Re=\infty$
0	0·332	0·422	0·472	0.491	0·498	0·5
0·1531	0·275	0·363	0·408	0·426	0·431	0·434
0·3889	0·219	0.299	0·338	0·353	0·358	0·360
0·7800	0·165	0·233	0·264	0·275	0·279	0·281
1·5000	0·114	0·164	0·187	0·196	0·199	0·200
3·0556	0·069	0·101	0.115	0·121	0·123	0·123
7·5000	0·032	0·048	0·055	0·058	0·058	0·059
31·5000	0·008	0·012	0·014	0·015	0·015	0·015

Table 2b. Pressure at the paraboloid

	$Re(1+Re^{1/2})^{-2}P(\xi, Re)$					
ξ/Re	$Re=1$	$Re=10^{-1}$	$Re=10^{-2}$	$Re=10^{-3}$	$Re=10^{-4}$	$Re=10^{-5}$
0	0·264	0·227	0·192	0·152	0·118	0·095
0·01	0·260	0·225	0·190	0·152	0·117	0·094
0·1	0·235	0·202	0·173	0·139	0·107	0·086
1	0·147	0·113	0·088	0·075	0·059	0·048
10	0·038	0·024	0·020	0·011	0·010	0·009
100	0·004	0·003	0·002	0·002	0·002	0·002

The pressure drag, i.e. the force in x-direction on the paraboloid caused by the pressure is given by

$$D_p = 2\pi \int_0^s rP^* \sin\gamma \, ds \tag{7.6}$$

where γ is the slope of the paraboloid surface and s is the curvilinear distance from the top along the surface. The dimensional pressure P^* is defined by $P^* = p - p_\infty$. Along the paraboloid we can write, using (2.4), $\sin\gamma \, ds = dr = \nu(Re/\xi)^{1/2} \, d\xi/U_0$ and the non-dimensional pressure drag coefficient becomes

$$C_{D_p} = \frac{D_p}{\rho v^2} = 4\pi Re \int_0^\xi P \, d\xi = 4\pi Re \int_0^\xi (P_N + P_S) \, d\xi$$

$$= 4\pi Re\left[\{Re(f''(Re) - f_0'''(Re)) - f_0''(Re)\}\ln\left(\frac{\xi + Re}{Re}\right) + 2f_0''(Re)\frac{\xi}{\xi + Re} + \int_0^\xi P_N \, d\xi\right] \tag{7.7}$$

The pressure drag coefficient tends to infinity as ξ grows without limit. Therefore we introduce a modified drag coefficient $\bar{C}_{D_p}$ by subtracting the leading term which is given by

$$4\pi Re\{Re(f''(Re) - f_0'''(Re)) - f_0''(Re)\}\ln \xi. \tag{7.8}$$

For $\bar{C}_{D_p}$ there remains at $\xi = \infty$

$$\bar{C}_{D_p}(\infty) = 4\pi Re\left[\{Re(f''(Re) - f_0'''(Re)) - f_0''(Re)\}\ln Re^{-1} + 2f_0''(Re) + \int_0^\infty P_N \, d\xi\right] \tag{7.9}$$

which is a finite value.

7.2. *Skin friction*

When τ denotes the shear stress, the local coefficient of skin friction is given by

$$C_f = \frac{\tau}{\frac{1}{2}\rho U_0^2} = \frac{2\nu}{U_0^2}\frac{\partial}{\partial n} v_\xi = \frac{2Re^{1/2}}{(\xi + Re)\xi^{1/2}} L(\xi, Re) \tag{7.10}$$

In this expression $(\partial/\partial n)v_\xi$ denotes the normal derivative of the dimensional velocity component v_ξ. Using (2.11) and (3.7b) we obtain

$$C_f = \frac{2(\xi Re)^{1/2}}{\xi + Re}\left\{f''(Re) + \frac{1}{\xi + Re} f_0''(Re) + \frac{1}{\xi} L_1(\xi, Re)\right\}. \tag{7.11}$$

In Tables 3a and 3b and in Fig. 3 we present values of $\frac{1}{2}(\xi + Re)(\xi Re)^{-1/2} C_f$ along the paraboloid surface. A normalization factor $Re(1 + Re^{1/2})^{-1}$ has been used. In Fig. 4 results for

Table 3a. Skin-friction at the paraboloid. $A = 1 + Re^{1/2}$

	$\frac{1}{2}A^{-1}(Re/\xi)^{1/2}(\xi + Re)C_f$				
ξ	$Re = 10$	$Re = 10^2$	$Re = 10^3$	$Re = 10^4$	$Re = 10^5$
0	0·598	0·775	0·871	0·989	0·921
0·1531	0·586	0·747	0·833	0·866	0·877
0·3889	0·571	0·714	0·787	0·816	0·825
0·7800	0·552	0·673	0·734	0·757	0·764
1·5000	0·528	0·626	0·673	0·690	0·696
3·0556	0·499	0·574	0·607	0·619	0·623
7·5000	0·466	0·519	0·541	0·548	0·551
31·5000	0·435	0·472	0·487	0·491	0·493
∞	0·421	0·452	0·464	0·468	0·469

Table 3b. Skin-friction at the paraboloid. $A = 1 + Re^{1/2}$

	$\frac{1}{2}A^{-1}(Re/\xi)^{1/2}(\xi + Re)C_f$					
ξ	$Re = 1$	$Re = 10^{-1}$	$Re = 10^{-2}$	$Re = 10^{-3}$	$Re = 10^{-4}$	$Re = 10^{-5}$
0	0·413	0·284	0·199	0·145	0·112	0·090
10^{-1}	0·413	0·284	0·199	0·145	0·112	0·090
1	0·410	0·282	0·198	0·145	0·111	0·089
10	0·390	0·277	0·197	0·144	0·111	0·089
10^2	0·365	0·272	0·196	0·144	0·111	0·089
∞	0·357	0·271	0·195	0·144	0·111	0·089

the skin friction in the nose are presented together with the values found by Davis and Werle [11]. For large Re these values should tend to the value assumed in first order boundary layer theory. This value is given by $G''(0)$, the function G being defined in (4.7). From the numerical solution of equation (4.7) we have $G''(0) = 0{\cdot}927680$. For small Re the Stokes approximation is valid. Therefore we present in Fig. 4 also the Stokes values of the presented quantity, which are found with the aid of the results of section 4.

The friction drag D_f can be written as

$$D_f = 2\pi \int_0^s r\tau \cos\gamma \, ds \tag{7.12}$$

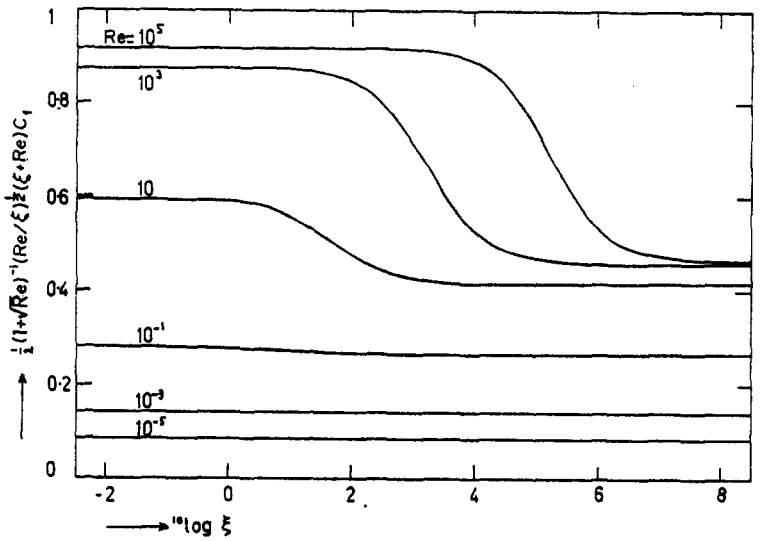

Fig. 3. Skin friction at the paraboloid surface.

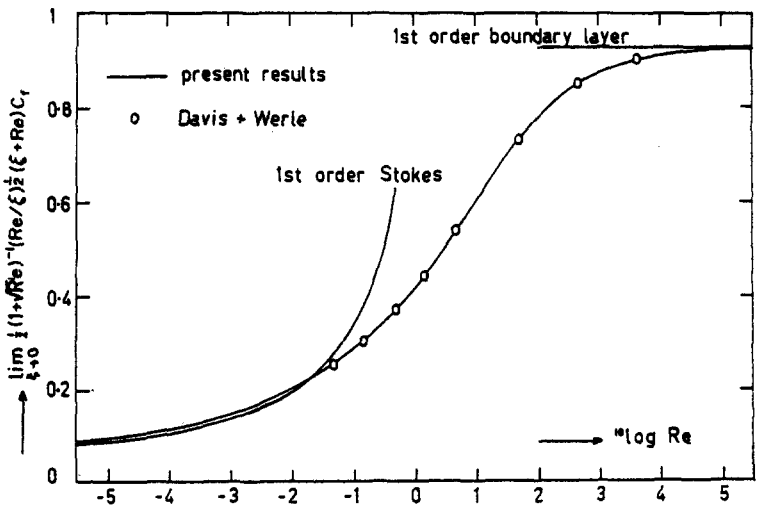

Fig. 4. Skin friction at the nose of the paraboloid.

Following the same reasoning as above for the pressure drag the non-dimensional friction drag coefficient is written in the form

$$C_{D_f} = \frac{D_f}{\rho v^2} = 2\pi \int_0^{\xi} (\xi Re)^{1/2} C_f \, d\xi.$$

With the aid of (7.11) this becomes

$$C_{D_f}(\xi) = 4\pi Re\left[f''(Re)\xi - \{Ref''(Re) - f_0''(Re)\}\ln\left(\frac{\xi + Re}{Re}\right) - f_0''(Re)\frac{\xi}{\xi + Re} + \int_0^{\xi} \frac{L_1}{\xi + Re}\, d\xi \right]. \quad (7.13)$$

We see that the friction drag coefficient also tends to infinity as $\xi \to \infty$. Again we subtract the leading terms, viz.

$$4\pi Re[f''(Re)\xi - \{Ref''(Re) - f_0''(Re)\}\ln \xi] \tag{7.14}$$

and we thus define a modified friction drag coefficient $\bar{C}_{D_f}$ which at $\xi = \infty$ has a finite value

$$\bar{C}_{D_f}(\infty) = 4\pi Re\left[\{Ref''(Re) - f_0''(Re)\}\ln Re - f_0''(Re) + \int_0^\infty \frac{L_1}{\xi + Re}\,d\xi\right]. \tag{7.15}$$

7.3. *The momentum theorem*

For the flow past a parabolic cylinder Botta, Dijkstra and Veldman [2] have derived an analytic expression for the drag coefficients with which these numerically calculated coefficients can be compared. This is also possible for flow past a paraboloid. We can derive the following equation

$$\frac{1}{2\pi}\{C_{D_f}(\xi) + C_{D_p}(\xi)\} = 2\xi Ref''(Re) + \beta^2 \ln \xi + M(Re) + 0(\xi^{-k_1}) \tag{7.16}$$

where

$$M(Re) = -2Re^2 f''(Re) + 2f_0(\infty) - \tfrac{5}{2}\beta^2 - \tfrac{1}{2}Re^2 + 3\beta Re - \beta - \beta^2 \ln Re - \int_{Re}^{\infty} [4f'f_0' + \{(\eta - \beta)^2 - f^2\}/\eta]\,d\eta$$

A derivation of this result is given by Veldman [13]. When we use (3.9) we see that the leading terms in (7.16) are produced by the sum of (7.8) and (7.14), that is they are generated by the subtracted terms. The first term to which the numerically computed quantities Ψ_1 and L_1 give a contribution is the term $M(Re)$. This term must satisfy the following equation

$$\frac{1}{2\pi}\{\bar{C}_{D_f}(\infty) + \bar{C}_{D_p}(\infty)\} = M(Re) \tag{7.17}$$

Table 4. The drag-coefficients and the total drag compared with the exact result from (7.17). $B = -2\pi(1 + Re^{1/2})^4$

Re	$\bar{C}_{D_f}(\infty)/B$	$\bar{C}_{D_p}(\infty)/B$	$\{\bar{C}_{D_f}(\infty) + \bar{C}_{D_p}(\infty)\}/B$ 32×128	extra-polated	$2\pi M(Re)/B$
10^{-5}	0·108	−0·002	0·106	0·115	0·122
10^{-4}	0·152	−0·002	0·150	0·160	0·161
10^{-3}	0·221	−0·003	0·218	0·225	0·229
10^{-2}	0·369	−0·015	0·354	0·366	0·372
10^{-1}	0·653	−0·056	0·597	0·608	0·610
1	0·974	0·111	1·085	1·094	1·097
10	0·892	1·383	2·275	2·276	2·277
10^2	0·518	3·790	4·308	4·312	4·312
10^3	0·234	6·465	6·699	6·701	6·701
10^4	0·094	9·012	9·106	9·108	9·108
10^5	0·035	11·431	11·467	11·469	11·469

In Table 4 the calculated values of $\bar{C}_{D_f}(\infty)$, $\bar{C}_{D_p}(\infty)$ and both sides of equation (7.17) are given. All values have been normalized by $(1 + Re^{1/2})^4$. For small Re there appeared

to be a large discretization error in the numerical calculated quantities, which causes the rather large discrepancy between the values of both sides of (7.17). To show that this discrepancy decreases when we use a finer grid we also present in Table 4 the values of the left hand side of (7.17) obtained with a Richardson extrapolation from the two finest grids based on a discretization error of $0(h^2)$. The extremely good agreement between both sides of equation (7.17) for large Reynolds numbers is caused by the fact that not only the pressure is approached by the contribution of the subtracted terms as $Re \to \infty$ (see equation (7.5)) but also the modified pressure drag $\bar{C}_{D_p}$. For details see Veldman [13].

Acknowledgements—The author wishes to express his gratitude to Prof. Dr. Ir. A. I. van de Vooren for his stimulating help and encouragement. He also wishes to thank Drs. D. Dijkstra and Drs. E. F. F. Botta for valuable advice. This work was supported by the Netherlands organization for the advancement of pure research (Z.W.O.).

APPENDIX

In Section 4 we have seen that for small Re the Oseen approximation gives a good description of the flow pattern. Therefore it may be expected that the Oseen approximation also gives good results for the eigenvalues mentioned in Section 3.

The eigenvalue equation (3.10) can be integrated once

$$\eta f_k''' + (f+1)f_k'' + (k+1)f'f_k' - kf''f_k = 0, \tag{A.1}$$

where the integration constant vanishes by reason of the boundary conditions for $\eta \to \infty$. For convenience we do not use the original Oseen approximation, i.e. a linearization around the oncoming flow, but we linearize around the potential flow past the paraboloid given by $\Psi = \xi(\eta - Re)$. Thus we substitute in equation (A.1) $f = \eta - Re$ and we obtain

$$\eta f_k''' + (\eta - Re + 1)f_k'' + (k+1)f_k' = 0.$$

In this equation we substitute $\eta = -x$ and $f_k'(\eta) = g(x)$, which results in

$$xg'' + (1 - Re - x)g' - (k+1)g = 0, \tag{A.2}$$

with boundary conditions $g(-Re) = 0$, $g(-\infty) = g'(-\infty) = 0$ exp.

Equation (A.2) is Kummer's equation and the full solution in the complex z-plane can be written as

$$g = C_1 {}_1F_1(k+1;\, 1-Re;\, z) + C_2 z^{Re} {}_1F_1(k+Re+1;\, 1+Re;\, z)$$

where C_1 and C_2 are constants, which can be evaluated by imposing the boundary conditions. First we examine the behaviour of g as $z \to \infty$, $\arg z = \pi$. This behaviour is given by (see [17], equation 13.5.1)

$$g \sim C_1 \Gamma(1-Re)\left\{\frac{e^{i\pi(k+1)} z^{-(k+1)}}{\Gamma(-Re-k)} A + \frac{e^z z^{k+Re}}{\Gamma(k+1)} B\right\} + C_2 z^{Re}\Gamma(1-Re)\left\{\frac{e^{i\pi(k+1+Re)} z^{-(k+1+Re)}}{\Gamma(-k)} A + \frac{e^z z^k}{\Gamma(k+1+Re)} B\right\} \tag{A.3}$$

where

$$A = \sum_{n=0}^{N-1} \frac{(k+1)_n (1+k+Re)_n}{n!} (-z)^{-n} + O(|z|^{-N})$$

and

$$B = \sum_{n=0}^{M-1} \frac{(-k)_n (-k-Re)_n}{n!} z^{-n} + O(|z|^{-M}).$$

The exponential decay of g now implies the cancelling of the first terms between the parentheses in (A.3). This yields

$$C_1 \frac{\Gamma(1-Re)}{\Gamma(-k-Re)} + C_2 e^{i\pi Re} \frac{\Gamma(1+Re)}{\Gamma(-k)} = 0. \tag{A.4}$$

Next we demand that $g(-Re) = 0$. Since Re is small we can develop $g(-Re)$ in a power series in Re

$$g(-Re) \sim C_1\left(1 - \frac{k+1}{1-Re} Re + O(Re^2)\right) + C_2(-Re)^{Re}\left(1 - \frac{k+Re+1}{1+Re} Re + O(Re^2)\right) \ldots$$

Further we have $(-Re)^{Re} = e^{i\pi Re}(1 + Re \ln Re + O(Re^2 \ln^2 Re))$. When we substitute this in the expansion for $g(-Re)$ and set $g(-Re) = 0$ we obtain

$$C_1 + C_2 e^{i\pi Re}(1 + Re \ln Re) = 0. \tag{A.5}$$

The two equations for C_1 and C_2, (A.4) and (A.5), must have a nontrivial solution hence we must set its determinant equal to zero

$$\Gamma(-k)\Gamma(1 - Re)(1 + Re \ln Re) = \Gamma(-Re - k)\Gamma(1 + Re). \tag{A.6}$$

Since Re is small we can develop $\Gamma(1 - Re)$, $\Gamma(1 + Re)$ and $\Gamma(-Re - k)$ in Taylor series whence equation (A.6) becomes

$$\frac{\Gamma'(-k)}{\Gamma(-k)} = -\ln Re + 2\Gamma'(1). \tag{A.7}$$

For the left hand side of (A.7) a series expansion is available ([17], equation 6.3.16) and $\Gamma'(1) = -\gamma$ where γ is Euler's constant, so we can transform (A.7) to

$$\sum_{n=0}^{\infty} \frac{-1-k}{(n+1)(n-k)} = -\ln Re - \gamma. \tag{A.8}$$

The error in (A.8) is of the order $Re \ln^2 Re$.

As Re approaches zero, $\ln Re$ grows without limit thus we conclude that $-k$ lies near a pole of $\Gamma(z)$. Suppose $k \approx m$, m integer, then the main contribution to the sum in (A.8) is given by the term with $n = m$. Setting this term equal to the right hand side of (A.8) we finally obtain

$$k = m - 1/\ln Re, \qquad m = 0, 1, 2, \ldots \tag{A.9}$$

with an error of the order $(\ln Re)^{-2}$. Thus we see that the eigenvalues tend to integers as Re tends to zero. This result is completely in agreement with the numerically calculated eigenvalues by Veldman [13].

REFERENCES

1. van de Vooren, A. I., and Dijkstra, D., The Navier–Stokes solution for laminar flow past a semi-infinite flat plate, *J. Eng. Math.* **4**, 9–27 (1970).
2. Botta, E. F. F., Dijkstra, D., and Veldman, A. E. P., The numerical solution of the Navier–Stokes equations for laminar, incompressible flow past a parabolic cylinder, *J. Eng. Math.* **6**, 63–81 (1972).
3. Smith, A. M. O., and Clutter, D. W., Solution of the incompressible laminar boundary layer equations, Douglas Aircraft Corp. Engng. Papers 1525 (1963).
4. Davis, R. T., Boundary layers on parabolas and paraboloids by methods of local truncation, *Int. J. Non-Linear Mech.* **5**, 625–632 (1970).
5. Mather, D. J., The motion of viscous liquid past a paraboloid, *Quart. J. Mech. Appl. Math.* **14**, 423–429 (1961).
6. Lee, L. L., Boundary layer over a thin needle, *Phys. Fluids* **10**, 820–822 (1967).
7. Cebeci, T., Na, T. Y., and Mosinskis, G., Laminar boundary layers on slender paraboloids, *AIAA J.* **7**, 1372–1374 (1969).
8. Miller, D. R., The boundary layer on a paraboloid of revolution, *Proc. Cambridge Philos. Soc.* **65**, 285–299 (1969).
9. Miller, D. R., The downstream solution for steady viscous flow past a paraboloid, *Proc. Cambridge Philos. Soc.* **70**, 123–133 (1971).
10. Tam, K. K., On the asymptotic solution of viscous incompressible flow past a heated paraboloid of revolution, *Siam J. Appl. Math.* **20**, 714–721 (1971).
11. Davis, R. T., and Werle, M. J., Numerical solutions for laminar incompressible flow past a paraboloid of revolution, *AIAA J.* **10**, 1224–1230 (1972).
12. Clark, D. C., The vorticity at infinity for solutions of the stationary Navier–Stokes equations in exterior domains, *Mathematics J.* **20**, 633–654 (1971).
13. Veldman, A. E. P., The numerical solution of the Navier–Stokes equations for laminar incompressible flow past a paraboloid of revolution, Report TW-122, Dept. of Math., University of Groningen (1972).
14. Greenspan, D., *Lectures on the Numerical Solution of Linear, Singular and Nonlinear Differential Equations*, Chapter 10, Prentice-Hall, Englewood Cliffs, New Jersey (1968).
15. Dennis, S. C. R., and Chang, G. Z., Numerical integration of the Navier–Stokes equations for steady two-dimensional flow, *Phys. Fluids Suppl. II* **12**, 88–93 (1969).
16. Blottner, F. G., and Flügge-Lotz, I., Finite difference computation of the boundary layer with displacement thickness interaction, *J. Mécanique* **2**, 397–423 (1963).
17. Abramowitz, M., and Stegun, I. A., ed., Handbook of Mathematical Functions, U.S. Department of Commerce, Washington D.C. (1964).